



AIAA 2000-4863

**Approximation of Probabilistic Distributions
Using Selected Discrete Simulations**

D. J. McCormick

J. R. Olds

Space Systems Design Laboratory

Georgia Institute of Technology

Atlanta, GA

**8th AIAA/USAF/NASA/ISSMO Symposium on
Multidisciplinary Analysis and Optimization**

**6-8 September 2000
Long Beach, California**

Approximation of Probabilistic Distributions Using Selected Direct Simulations

David J. McCormick[†]

Dr. John R. Olds^{††}

Space Systems Design Laboratory

School of Aerospace Engineering

Georgia Institute of Technology, Atlanta, GA 30318-0150

ABSTRACT

The goal of this research is to find a computationally efficient and easy to use alternative to current approximation or direct Monte Carlo methods for robust design. More specifically, a new technique is sought to use selected deterministic analyses to obtain probability distributions for analyses with large inherent uncertainties.

Two techniques for this task are investigated. The first uses a design of experiments array to find key points in the algorithm space upon which deterministic analyses will be performed. An expectation value error minimization routine is then used to assign discrete probabilities to the individual runs in the array based on the joint probability distribution of the inputs. This creates a representative distribution that can be used to estimate expectation values for the output distribution.

The second technique uses a similar error minimization algorithm, but this time alters the location of the points to be sampled from the function space. This means that for every change in input variable distribution, the algorithm will generate a table of runs at input locations that minimize the error in expectation values.

The advantages of these techniques include a small time savings over approximation or direct Monte Carlo methods as well as elimination of numerical noise due to random number generation. This noise will be shown to be a hindrance when converging multiple Monte Carlo analyses. In addition, when the variable location sampling point algorithm is used, this takes away the arbitrary task of defining levels for the input variables and provides enhanced accuracy.

NOMENCLATURE

CA	contributing analysis
CCD	central composite design
c.g.	center of gravity
DP	discrete probability
EC&D	electric conversion and distribution
FPI	Fast Probability Integration
GLOW	gross liftoff weight
I_{sp}	specific impulse
ISS	International Space Station
KSC	Kennedy Space Center
MC	Monte Carlo
MR	mass ratio (liftoff mass / burnout mass)
OMS	orbital maneuvering system
p_f	propellant mass fraction
POST	Program to Optimize Simulated Trajectories
RCS	reaction control system
RSE	response surface equation
SSTO	single stage to orbit
T_{vac}	vacuum thrust
TRF	technology reduction factor
$\hat{\mu}$	sample mean
$\hat{\sigma}$	sample standard deviation

INTRODUCTION

Background and Motivation

Current aerospace vehicle conceptual multi-disciplinary design is typified by deterministic design methods. These methods ignore important design uncertainty information. Designers are often required to make a "best guess" estimate of a key design parameter thus losing critical knowledge of the range of uncertainty that might be present in a subsequent dataset. Conceptual launch vehicle design (Fig. 1) is one area particularly interested in this design uncertainty (Ref. 1.)

Risk is one type of information that is important to know, yet is usually not quantified. Risk in this case refers to the effect of uncertainty on the

[†] - Graduate Research Assistant, School of Aerospace Engineering, Student member AIAA.

^{††} - Assistant Professor, School of Aerospace Engineering, Senior member AIAA.

performance of a design. When program planning and risk reduction activities are undertaken for an aerospace project, knowing the amount and sources of risk in a design should result in more efficient programs.

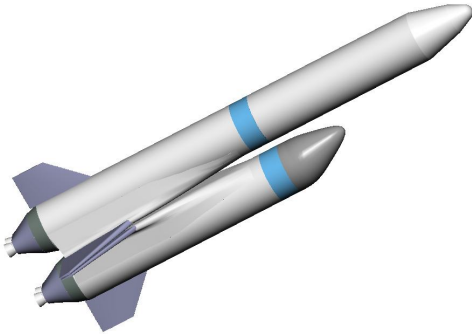


Figure 1 – Example of Reusable Launch Vehicle Conceptual Design

Another related quantity is design maturity. By carrying through appropriate levels of uncertainty in the design, appropriate confidence in that design's performance can be expressed. This brings more realism and a heightened awareness of the lack of design maturity to conceptual design.

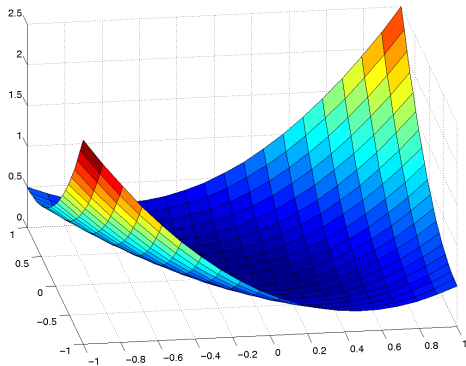


Figure 2 – Response Surface Equation

Current methods for robust conceptual design are typically direct Monte Carlo (MC) methods either operating directly on an engineering simulation or an a fast approximation of the true engineering simulation. The latter is called a “meta-model” and is typically a polynomial approximation or response surface equation fit to selected data produced by the true engineering simulation (Fig. 2.) Monte Carlo methods use random inputs selected from assumed input distributions to

obtain estimates of the output distributions and associated statistical characteristics. The MC analysis must be run on the order of 10,000 times to obtain output distributions.

To convey probabilistic information, a meta-model must still be combined with a Monte Carlo simulation and again numerical noise is present due to the use of pseudo-random number generation.

Research Goal

The goal for this research is to create a new method for probabilistic analysis that improves on current techniques. This new method should be fast, accurate and has low numerical noise. While speed and accuracy are obviously positive attributes, the goal for the method to have low numerical noise is so that it can be useful in an iterative multidisciplinary design environment. The generation of gradients is on task that requires low noise.

METHODOLOGY

Overall Concept

The technique presented consists of selecting a small number of discrete points representing samples from an input probability distribution and use them in a deterministic engineering simulation to approximate the entire resultant output probability distribution. Key statistical parameters (mean, standard deviation, etc.) are also desired.

The first step is to represent the input distribution as discrete points. Each of these points has a probability associated with it. Both the location and probability values can be selected so as to either minimize or drive to zero the error in selected expectation values between the discrete points and the actual distribution.

The expectation value of a function $E(g(x))$ is the weighted mean of $g(x)$ where the weights are the probabilities of each point x in a discrete distribution (Ref. 2.)

Fig. 3 shows a one-dimensional example of the point selection process. These points can be used to find expectation values that represent important properties of the input distribution, such as mean, standard deviation and skew. Higher accuracy in the input distribution model should translate to higher accuracy in the output distribution model.

Because the probability of a set of inputs occurring is equal to the probability of the associated result occurring, the probabilities of each of the outputs is known. These discrete points can then be evaluated to obtain estimates of the output distribution properties using the expectation values of the discrete output distributions. Again, these can include mean, variance, skew, etc. It is important to note that these properties have been obtained non-stochastically and should have low numerical noise.

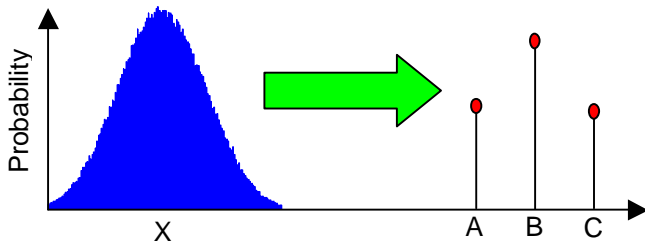


Figure 3 – Discrete Point Representation of an Input Distribution

Fixed-Location Method

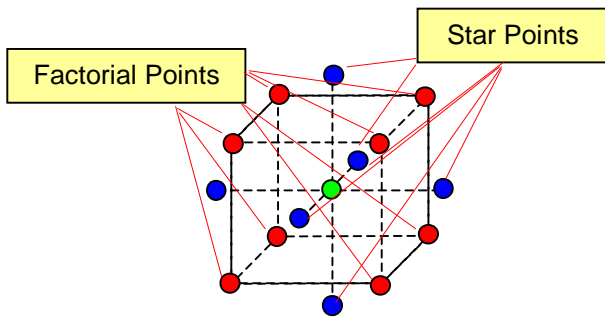


Figure 4 – Three Variable Central Composite Design

The first technique to be introduced for this paper is a fixed-location method. It utilizes a central composite design (CCD) experiment array to determine the sampling point locations for the input distribution model. A three dimensional example of the sampling points is shown in Fig. 4. The cube corners form a two level full factorial, while the points radiating from the center are referred to as “star points.” These typically extend past the upper and lower bounds of the two-level full factorial. This central composite should span an appropriate amount of the input distribution variables so that a reasonably accurate representation of the distribution is possible.

The input distribution properties are then matched by varying the probabilities of the individual points in the discrete model. The technique used for this is analogous to least squares curve fit matching. The problem statement for this is given in Equation 1.

$$\text{Min}_{\vec{p}} \|A\vec{p} - \vec{E}\|_2 \quad (1)$$

The \vec{E} vector contains expectation values for polynomial terms corresponding to the properties of the input distribution. It expresses the properties of the input distribution. It is important that one of the g polynomial terms be unity so that the probabilities of the points in the model add up to one. The matrix A contains the locations of the points in the model expressed in rows corresponding to the polynomial terms expressed in \vec{E} . A description of these arrays is found in Equations 2 and 3. The columns of A correspond to each of the m sample points. The \vec{p} vector contains the probabilities of each of the m points in the model to be determined by the minimization.

$$\vec{E} = \begin{bmatrix} E(g_1(\vec{x})) \\ E(g_2(\vec{x})) \\ \vdots \\ E(g_n(\vec{x})) \end{bmatrix} \quad (2)$$

$$A = \begin{bmatrix} g_1(\vec{x}_1) & g_1(\vec{x}_2) & \dots & g_1(\vec{x}_m) \\ g_2(\vec{x}_1) & g_2(\vec{x}_2) & & g_2(\vec{x}_m) \\ \vdots & & \ddots & \vdots \\ g_n(\vec{x}_1) & g_n(\vec{x}_2) & \dots & g_n(\vec{x}_m) \end{bmatrix} \quad (3)$$

The vector \vec{p} is found using a QR factorization minimization of the form shown in Equations 4 - 7.

$$\text{Min}_{\vec{p}} \|A \vec{p} - \vec{E}\|_2 = \text{Min}_{\vec{p}} \|QR\vec{p} - \vec{E}\|_2 \quad (4)$$

$$\text{Min}_{\vec{p}} \|QR\vec{p} - \vec{E}\|_2 = \text{Min}_{\vec{p}} \|Q(R\vec{p} - Q^T \vec{E})\|_2 \quad (5)$$

Because Q is orthogonal, Equation 5 is equivalent to Equation 6.

$$\text{Min}_{\vec{p}} \left\| \begin{pmatrix} (Q^T \vec{E})_{1...n} \\ (Q^T \vec{E})_{n+1...m} \end{pmatrix} - \begin{pmatrix} R\vec{p} \\ 0 \end{pmatrix} \right\|_2 \quad (6)$$

so

$$R\vec{p} = (Q^T \vec{E})_{1...n} \quad (7)$$

solves the minimization. This is because the only variable is the \vec{p} vector and it cannot affect the $(n+1)^{\text{th}}$ through m^{th} equations. Also, to avoid singularity problems, it is important that the polynomial terms chosen for use as expectation values be linearly independent and that sample points are not repeated in the discrete model.

Once the probabilities are determined, the sample points can be evaluated. This gives the response and each of the corresponding probabilities. For the three dimensional CCD shown in Fig. 4, a sample response distribution would resemble Fig. 5. Note that each of the input point probability values corresponds to a value for the response.

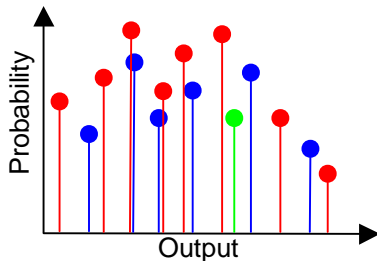


Figure 5 – Final Output Response of a Fixed Location Discrete Probability Method Using a Central Composite Design

Variable Location Method

The second technique for this paper uses both variable sample point locations and probabilities in its input distribution model. This has an advantage in that the user does not need to arbitrarily set the locations of the sample points. It also has the advantage of additional degrees of freedom when minimizing the error to the target input distribution expectation values. This means that more distribution matching accuracy can be carried through the analysis with fewer points when compared to the fixed location method.

For this method, the input distributions are assumed to be independent. This simplifies identifying sample points a great deal. Each of the sample point

settings can be found independently for each variable’s input distribution, then combined to form a full-factorial design. This idea is illustrated in Figure 6.

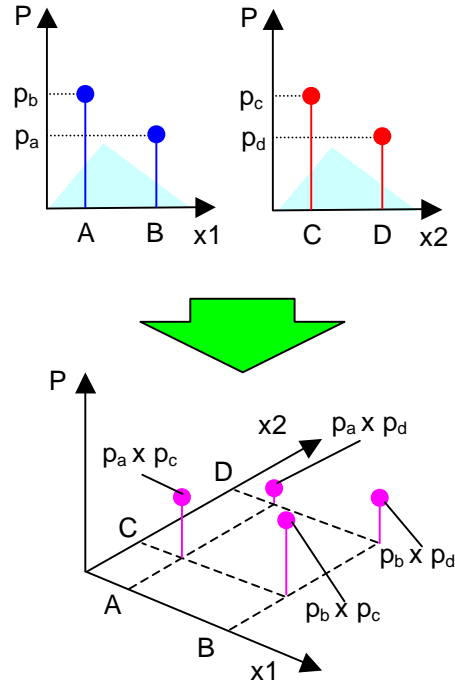


Figure 6 – Variable Location Point Generation

For each of the variable input distributions, the locations and probabilities of the sample points must be determined. In order to maximize the amount of input distribution property information carried through the analysis, this particular method drives the error in the selected expectation values to zero.

For each of the variables, there are four degrees of freedom. That means that all expectation values up to cubic can be matched by the method. Consequently, mean, variance and skewness can all be represented. The problem to be solved to find the location and probabilities of the sample points is defined by Equations 8 and 9.

$$\vec{f} = \begin{pmatrix} p_1 + p_2 - 1 \\ p_1 x_1 + p_2 x_2 - E(x_{inputdist}) \\ p_1 x_1^2 + p_2 x_2^2 - E(x_{inputdist}^2) \\ p_1 x_1^3 + p_2 x_2^3 - E(x_{inputdist}^3) \end{pmatrix} = \vec{0} \quad (8)$$

This is equivalent to:

$$\vec{f} = \begin{pmatrix} p_1 x_1 + (1 - p_1) x_2 - E(x_{inputdist}) \\ p_1 x_1^2 + (1 - p_1) x_2^2 - E(x_{inputdist}^2) \\ p_1 x_1^3 + (1 - p_1) x_2^3 - E(x_{inputdist}^3) \end{pmatrix} = \vec{0} \quad (9)$$

From this point, a Newton-Rhaphson multivariate root finding method is employed to solve the nonlinear set of equations. As a practical note, initial guess is very important. For most cases encountered by this study, an initial guess of the mean plus and minus one standard deviation is sufficient for x_1 and x_2 , the high and low sample points. An initial guess of 50% for p_1 is also effective.

Once the inputs are combined to form a two-level full factorial design (Fig. 6.) the deterministic analysis finds the response corresponding to each of the sample points. Again the input probabilities are used along with this response to find the output parameters of interest.

Model for Launch Vehicle Sizing

For a test of these methods, an iterative sizing algorithm is used. Because probabilistic sizing is different from deterministic sizing, definition and description of this algorithm is required.

In this case, a simple two-analysis sizing technique is used. The first contributing analysis (CA) is Weights and Sizing. In a deterministic environment, this analysis changes the mold-line size of the launch vehicle until the vehicle’s mass ratio (MR) matches the mass ratio reported by the trajectory analysis. This is commonly done photographically so as to minimize the aerodynamic coefficient change between iterations. Stage MR is related to stage propellant mass fraction (p_f) by Equation 10. For high propellant fraction vehicles, MR is a more convenient metric and will be used from this point forward.

$$\frac{mass_{liftoff}}{mass_{burnout}} = MR = \frac{1}{1 - p_f} \quad (10)$$

For probabilistic analysis, it is still convenient to use the vehicle size as a control variable. However, a probabilistic trajectory analysis yields a distribution of MR, not a single value. There are also internal uncertainties in the weights and sizing analysis that yield a probability distribution of available MR.

To reconcile this problem, an error variable is created that is the difference of the available and required MR’s. At this point a decision must be made as to the desired confidence level of the analysis. This number should be related to the acceptable program risk. Using the decided confidence level, the size of the vehicle is altered until the percentile corresponding to the desired confidence level of MR error is driven to zero (Fig. 7.) For example, a 90% confidence level corresponds to a 90% chance that this size vehicle will either meet or exceed mission requirements.

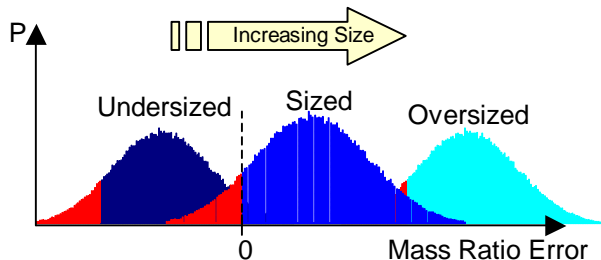


Figure 7 – Probabilistic Weights and Sizing Algorithm

The probabilistic trajectory analysis is more straightforward. Here, internal uncertainty variables are combined with the distributions reported from weights and sizing to generate a distribution of optimized MR. A diagram of this iteration is in Fig. 8.

This system is iterated until the MR_required distribution converges.

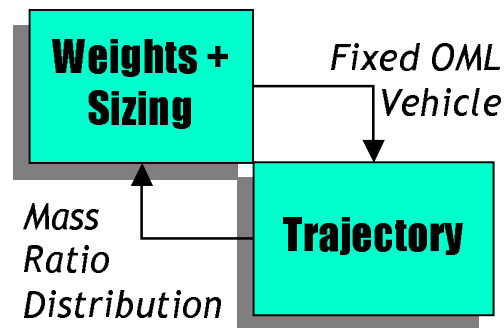


Figure 8 – Conceptual Sizing Iteration

TEST PROCEDURE AND RESULTS

To test these methods, two separate examples were run. The first involved a single deterministic analysis to compare the accuracy of several methods. The second was an iteration test to primarily determine the importance of noise in probabilistic

multidisciplinary sizing. This test also provides a practical example of probabilistic sizing. This section describes the procedure and results of both tests.

Single Analysis Test

One relatively computationally intensive part of conceptual launch vehicle design is trajectory analysis. Because of this, it is an ideal candidate for testing probabilistic approximation methods. Program to Optimize Simulated Trajectories (POST, Ref. 3) was used for this test. The trajectory for testing was a three dimensional, single-stage-to-orbit (SSTO) rocket traveling to an International Space Station (ISS) transfer orbit. Fig. 9 illustrates this.

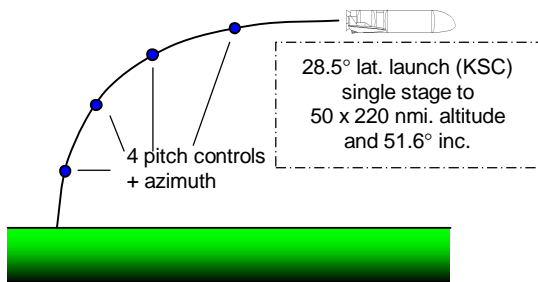


Figure 9 – Test Trajectory Parameters

Three noise variables were selected for the test. They were:

- Drag: a multiplier on the vehicle drag to reflect uncertainty in vehicle aerodynamic coefficients.
- Vacuum thrust (T_{vac}): a multiplier on the vehicle vacuum thrust to simulate possible engine underperformance.
- I_{sp} : varied to reflect uncertainty in engine efficiency.

These variables were given triangular input distributions corresponding to Table 1. For this type of distribution, the probability density varies linearly from zero at the minimum and maximum to a most likely point somewhere between the min and max.

Table 1 – Trajectory Input Distributions

	Minimum	Most Likely	Maximum
Drag Mult.	80%	100%	120%
Thrust Mult.	95%	100%	105%
I_{sp}	449 sec	451.5 sec	453 sec

Monte Carlo Analysis

Four different simulations were performed. First was a direct Monte Carlo analysis on POST. This was used as the reference for the other approximation methods. This technique was chosen as a reference because it did not rely on an approximation assumption for analysis. Because of this, it was the most straightforward analysis, but also the most computationally intensive. First, a table of 10,000 randomly selected input settings from the distributions described above were generated. Next, these randomly generated points were run and the output properties measured.

Response Surface – Monte Carlo Analysis

The first approximation method tested was and is a common technique for robust simulation. The first step was to create a meta-model of the analysis. In this case, a quadratic response surface equation was created for the three noise variables. This was accomplished by sampling from a CCD and then performing a least-squares curve fit on the results.

Next, a 10,000 run Monte Carlo analysis was run on the RSE. Output distribution properties could then be calculated in the same manner as in the direct Monte Carlo test.

Fixed-Location Sampling Method

The first of the new methods tested for this paper was the fixed-location discrete probability technique. For sampling points, this used the same CCD as the Response Surface – Monte Carlo technique. Equation 10 shows the expectation values that were used for input distribution probability matching. The \vec{E} vector is explained in the previous section on methodology.

$$\vec{E} = \begin{bmatrix} E(1) = 1 \\ E(x_1) \\ E(x_2) \\ E(x_3) \\ E(x_1x_2x_3) \\ E(x_1x_2) \\ E(x_1x_3) \\ E(x_2x_3) \\ E(x_3^2) \\ E(x_2^2) \\ E(x_1^2) \end{bmatrix} \quad (10)$$

Variable Location Method

The variable location method was executed as described in the methodology section with no additional assumptions. The uncertainty variables were identical to the other tests.

Single Analysis Test Results

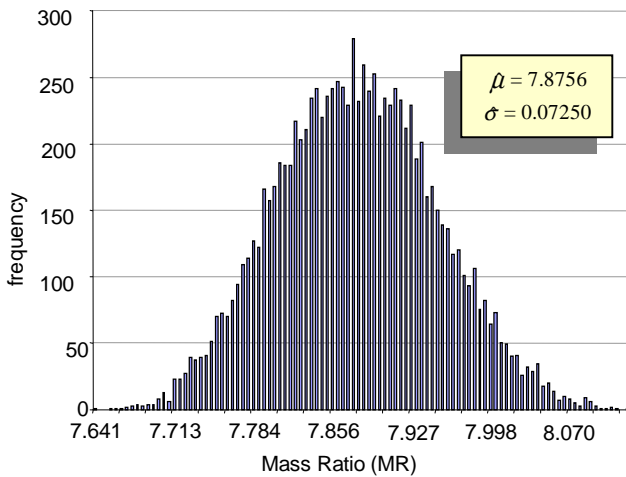


Figure 11 – Direct Monte Carlo Test Results

The first step is to gauge the reference distribution. Fig. 11 shows the output MR distribution for a direct Monte Carlo simulation. It should be noted that this required 10,000 fully optimized trajectory runs, and for most organizations is too computationally intensive a technique for use in a fast-response multidisciplinary environment. For example, the analysis for this paper took approximately eight days using two SGI Octane workstations running in parallel.

This test seems to show reasonable MR numbers as well as a well-formed distribution. The values of mean and standard deviation shown in the corner indicate the target values for the other analyses.

Response Surface – Monte Carlo Analysis Result

Figs. 12 and 13 show a reasonable correlation between the response surface and the direct analysis when it comes to approximating the mean of the distribution. However, it is slightly less accurate at measuring standard deviation than the two discrete sampling point methods. Fig. 13 shows a normal distribution probability density function (PDF) plotted using the test results for mean and standard deviation.

The RSE method is not discernable from the direct Monte Carlo in this context.

Because the RSE can be quickly calculated, it might make sense to do more than 10,000 runs to try to improve the accuracy of the technique. One consideration is that 10,000 runs on the polynomial response surface does take on the order of 30 seconds using a 500 megahertz Pentium III IBM-compatible PC. Increasing this would increase this time to a point where the expense of the method would not really be comparable to the others, which have negligible post-processing expense. Increasing to 30,000 runs does improve the accuracy, but it is still not as close on standard deviation as the two-level variable location discrete probability method.

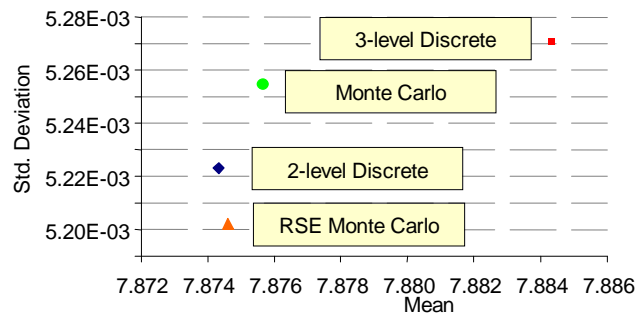


Figure 12 – Plot of Mean MR vs. Standard Deviation

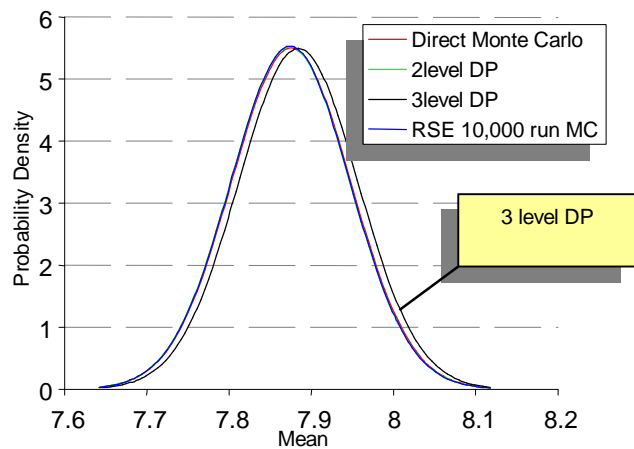


Figure 13 – Normal Distribution Probability Density Function of Test Results

Fig. 13 puts these results in perspective, however. As evidenced by the plotted normal distribution approximation for all of the methods, the RSE – MC

method is one of the techniques that falls on top of the direct Monte Carlo distribution in this figure. The difference in standard deviation is not visible from this perspective.

Variable Location Test Result

This technique is the closest to the Monte Carlo reference distribution. Figs. 12 and 13 show this clearly. It has both good mean and standard deviation accuracy while at the same time requiring the fewest number of runs.

The major disadvantage of this technique is that it requires re-running the deterministic analysis sampling set every time the input distributions change. This is acceptable for a “once-through” analysis, but could become cumbersome in an iterative situation.

However, due to its low number of sample points and high accuracy, this is still a powerful tool for many situations. Even iterative analyses might still make use of this technique if alternatives have noise that is too high.

Fixed Location Test Result

There appears to be significant error in the mean of the output distribution using the fixed location method. The cause of this error is not readily identifiable, and otherwise the method appears to be accurate. This distribution is the offset curve in Fig. 13. One advantage is that it is the closest in standard deviation, however as Fig. 13 illustrates, this is not enough to make up for its mean error.

Table 2 –Results of Single Analysis Test

	POST runs	MR mean	MR std. dev.
Direct Monte Carlo	10,000	7.8756	5.2558x10 ⁻³
RSE – Monte Carlo	15	7.8745	5.2033x10 ⁻³
Rel. error from MC		0.014 %	1.0 %
2 level discrete prob.	8	7.8742	5.2241x10 ⁻³
Rel. error from MC		0.018 %	0.60 %
3 level discrete prob.	15	7.8843	5.2714x10 ⁻³
Rel. error from MC		0.11 %	0.30 %

If the accuracy can be improved, this should be a very powerful tool for iterative analysis. While it requires more runs than the variable location method, it

does not need to be rerun, as long as the input distributions are within the range of the original sample points. In this way, it is similar to response surface methods, but with less iterative noise. This could be a great advantage in future iterative systems.

Iteration Test

An example launch vehicle was sized to determine the suitability of probabilistic analysis in a multidisciplinary environment.

The vehicle sized was a wing-body reusable rocket third generation technology SSTO. The concept is a simple wing-body with a cylindrical propellant tanks and oxidizer tank aft layout. It features five high thrust-to-weight ratio liquid oxygen/ liquid hydrogen (LOX/LH2) rocket engines mounted in a cluster at the rear of the craft. The payload is carried centrally, near the vehicle center of gravity (c.g.), giving it a small c.g. travel between payload-in and payload-out conditions. Other design features include wingtip mounted fins for lower induced drag and greater control authority, cylindrical tanks with elliptical domes for low structural weight and a set of hydrogen ducted fan landing engines for landing abort capability.

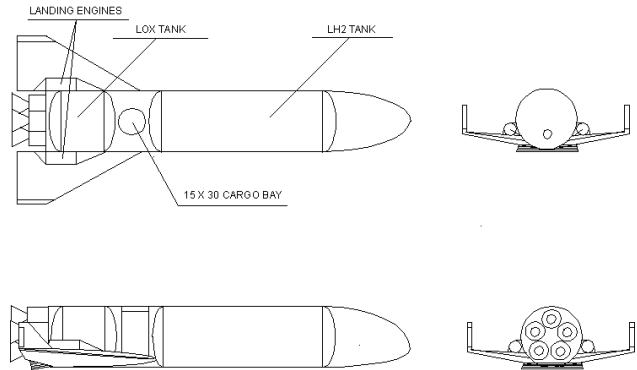


Figure 10 – Example Vehicle For Iteration Test

For the iteration test, the sizing algorithm described in the methodology section was used. More specifically for the Weights and Sizing analysis, a direct Monte Carlo simulation was used. There were two reasons for this decision.

First, there were thirty uncertainty variables. These are described in the Appendix. This would mean over a billion runs if any of the approximation methods mentioned above were to be used.

Second, using the Monte Carlo would test the hypothesis that the noise in a Monte Carlo analysis would hinder convergence in a multidisciplinary system.

For the trajectory analysis, the variable location discrete probability sampling method was used. Because of the lower level of uncertainty than the weights and sizing, an approximation method could be used. As will be shown later, this sampling method proved to be the most accurate. The trajectory analysis was identical to the one in the single analysis test, except for the inclusion of a probability distribution for gross liftoff weight (GLOW.)

Iteration Test Results

The main interests in the results of this test are convergence speed and numerical noise caused by iterating probabilistic analyses.

Fig. 14 shows a convergence rate similar to deterministic analyses. However, what is more difficult to see is the noise in the solution. Iterations three and four do not have changes that are discernable by the root finding method used to size the vehicle. This is due to noise in the Monte Carlo analysis. This creates a problem because the MR distribution has not yet converged to the level of precision (five significant figures) typically expected of the deterministic version of this sizing exercise. It had only achieved three significant figures of convergence at this point.

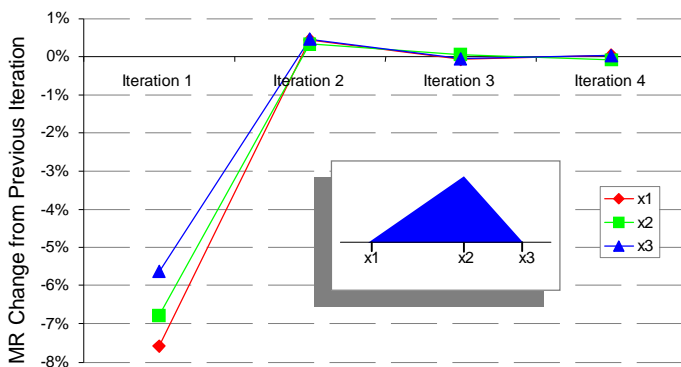


Figure 14 – Convergence History of Iteration Test

Table 3 – Iteration History

Mass Ratio Distribution				
Iter.	Minimum	Most Likely	Maximum	Avg. % Change
0	8.3	8.4	8.5	N/A
1	7.6714	7.8299	8.0214	6.7%
2	7.7057	7.8559	8.0584	0.41%
3	7.7008	7.8605	8.0542	0.058%
4	7.7042	7.8537	8.0566	0.053%

This illustrates both an advantage and a problem with Monte Carlo based probability analysis. The advantage is that many times, the number of variables is so large that most organized sampling methods simply explode in the number of runs required. The disadvantage is noise.

Table 4 – Final Results of Iteration Test

	Mean	Std. Dev.
Dry Weight	168,405 lb.	3,679 lb.
Gross Liftoff Weight	1,726 Klb.	4,263 lb.
Length	149 ft.	N/A
Width	30 ft.	N/A
Wingspan	102 ft.	N/A
Mass Ratio	8.0633	0.1296

The types of results this analysis can generate are shown in Fig. 15 and Table 4. These show distributions for the vehicle weights, and a single value for the vehicle’s physical dimensions. This is due to the sizing technique discussed before.

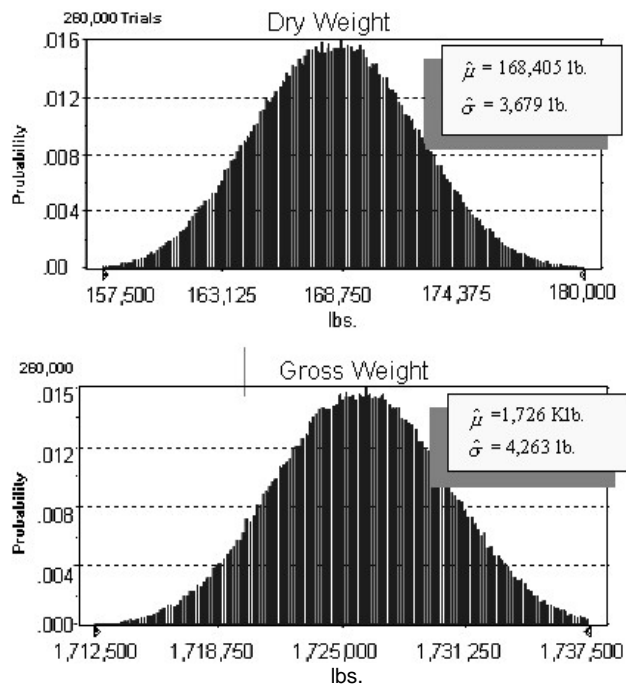


Figure 15 – Weight Results of Iteration Test

CONCLUSIONS

Several conclusions can be drawn from the results of the tests generated above.

1. Two new methods for determining the uncertainty through deterministic analyses were presented. Along with them, two examples were given for the use of these methods. Useful information about the robustness of a launch vehicle concept was extracted and the one of the methods was tested in practical application.
2. This technique promises to remove the burden of overly precise WER's, provided they can be interfaced with other probabilistic methods. This should also yield appropriate risk information.
3. The variable location discrete probability method was shown to have advantages in speed, accuracy and generality. Generality was shown in that the technique required little definition before it could be adapted to the example problems.
4. Numerical noise was shown to be an issue with iterative stochastic analyses. It proved to be a hindrance to convergence to the desired level of

precision. Potential ways of solving this problem are presented in the Future Work section of this paper.

5. Currently, problems with large uncertainty cause sampling schemes that are too large. One possible way to reduce this number would be a screening array to find the variables that contribute most to the response.

FUTURE WORK

1. Find a way to improve the accuracy of the fixed location discrete probability sampling method. There are a number of ways to improve this estimate, such as changing the expectation value model, experiment design, etc.
2. Find a way to reduce the number of sample points required for large problems. This the major disadvantage of all the approximation methods presented in this paper.
3. Test other probability estimating techniques, such as Fast Probability Integration (FPI, Ref. 4) for their applicability to launch vehicle systems design. This should be done in a fully iterative environment with an eye to computational expense.
4. Test the discrete probability sampling technique on problems other than trajectory. This should reveal additional advantages and disadvantages to the different methods.
5. Attempt to integrate this method into several multidisciplinary design environments, including Collaborative Optimization (Ref. 5), Optimization Based Decomposition, etc.

REFERENCES

1. McCormick, David J. and Olds, John R., "System Robustness Comparison of Advanced Space Launch Concepts," AIAA paper 98-5209, October 1998.
2. Hogg, R. V., and Tanis, E. A., *Probability and Statistical Inference, 4th Ed.*, Prentice-Hall, Inc., Englewood Cliffs, NJ, 1993.
3. Brauer, G. L., Cornick D. E., and Stevenson, R., "Capabilities and Applications of the Program to Optimize Simulated Trajectories," NASA CR-2770, February, 1977.
4. Mavris, D.N., Mantis, G., Kirby, M.R., "Demonstration of a Probabilistic Technique for the Determination of Economic Viability," SAE-975585, 1997.
5. Braun, R. D., Moore, A. A. and Kroo, I. M., "Collaborative Approach to Launch Vehicle Design," *Journal of Spacecraft and Rockets*, Vol. 34, No. 4, 1997, pp. 478-486.

Appendix – Weights and Sizing Uncertainty Assumptions

	Minimum	Most Likely	Maximum	Description
EC&D %age of Dry Wt.	5.58%	6.2%	6.82%	Electrical Conversion and Distribution percentage of dry weight.
Surface Control Actuation % of Entry Weight	0.432%	0.480%	0.528%	Aerodynamic Surface Control Weight
Residual OMS/RCS %age	4.5%	5%	5.5%	percentage of OMS and RCS propellant left after use.
Main Propellant residuals	0.45%	0.5%	0.55%	Percentage of Main propellant left after as unusable.
OMS/RCS reserves	9%	10%	11%	Reserve on-orbit maneuver propellant.
RCS %age of Entry Wt.	.302%	.336%	.370%	Reaction control system weight as a percentage of entry weight.
OMS Isp	455s	463s	470s	Efficiency of the Orbital Maneuvering System.
RCS Isp	420s	440s	462s	Efficiency of the Reaction Control System
Ascent Reserve and Unusable	0.45%	0.5%	0.55%	Ascent Reserve propellant as a percentage of ascent propellant
Inflight Losses and Vents	0.9%	1.0%	1.1%	Inflight propellant and pressurant losses as a percentage of ascent propellant
Tank Ullage	2.25%	2.50%	2.75%	Percent of tank volume that is unfillable.
Start up % of Ascent Propellant	0.9%	1%	1.1%	Engine startup propellant expended before liftoff
Primary Structure Wt. Per Unit Area	2.45 lb/ft ²	3.20 lb/ft ²	3.94 lb/ft ²	Load bearing structural elements
Secondary Structure Wt. Per Unit Area	1.12 lb/ft ²	1.25 lb/ft ²	1.37 lb/ft ²	Light-load bearing structural elements
LOx Tank Wt. / Volume	0.509 lb/ft ³	0.566 lb/ft ³	0.680 lb/ft ³	Liquid oxygen tank weight per unit volume
LH2 Tank Wt. / Volume	0.353 lb/ft ³	0.392 lb/ft ³	0.431 lb/ft ³	Liquid hydrogen tank weight per unit volume
Body Flap Wt. / Area	2.257 lb/ft ²	2.900 lb/ft ²	3.637 lb/ft ²	Body Flap weight per unit volume.
Exposed Wing TRF	36%	40%	46%	Percentage technology reduction factor for the exposed wing structure weight.
Wing Carry Through TRF	36%	40%	46%	Percentage technology reduction factor for the internal wing structure weight.
Tail TRF	36%	40%	46%	Percentage technology reduction factor for the tail weight
Thrust Structure TRF	23%	30%	37%	Percentage technology reduction factor for the thrust structure weight.
Payload Bay Structure %age	7%	15%	24%	Percentage of payload weight
ACC Panel Unit Weight	1.62 lb/ft ²	1.80 lb/ft ²	2.34 lb/ft ²	Weight per unit area for nose Thermal Protection System (TPS)
TUFI Tile Unit Weight	1.17 lb/ft ²	1.30 lb/ft ²	1.69 lb/ft ²	Weight per unit area for windward side TPS
TABI Blanket Unit Weight	0.72 lb/ft ²	0.80 lb/ft ²	1.04 lb/ft ²	Weight per unit area for leeward side TPS
Primary Power Weight per Day	125.6 lb	139.6 lb	153.6 lb	Power generation for launch vehicle per mission day.
Avionics Weight	1,440 lb	1,600 lb	1,760 lb	Weight of avionics
Environmental Control Multiplier	0.90	1.00	1.10	Multiplier on the weight of the environmental control system.
Landing Ducted Fan Isp	12,000s	16,000s	20,000s	Fuel efficiency of the ducted fan for powered landing.